9166 *Macromolecules* **2006,** *39,* 9166−9170

Polymer/Gas Clathrates for Gas Storage and Controlled Release

Loredana Annunziata,† Alexandra R. Albunia,† Vincenzo Venditto,†
Giuseppe Mensitieri,‡ and Gaetano Guerra*,†

Dipartimento di Chimica, Università di Salerno, via Ponte Don Melillo, I-84084 Fisciano (Salerno), Italy, and Dipartimento di Ingegneria dei Materiali e della Produzione, Università di Napoli "Federico II", Piazzale Tecchio, 80125 Napoli, Italy

Received August 16, 2006; Revised Manuscript Received October 4, 2006

ABSTRACT: The nanoporous crystalline phase of a cheap commercial polymer shows, already at room temperature, large uptake of gas molecules (e.g., butadiene and carbon dioxide) leading to polymer/gas clathrate phases. These clathrate phases have been characterized by X-ray diffraction and infrared linear dichroism measurements. Gas release kinetics are strongly reduced as a consequence of clathrate formation and can be further reduced by (010) orientation of the host phase, i.e., by placing the *ac* layers of close-packed enantiomorphous polymer helices nearly parallel to the film plane. The reported results indicate that this robust and easy-to-process polymeric crystalline framework is suitable for gas storage and controlled release.

The improvement of gas storage, recognition and separation techniques represents a strategic industrial and environmental objective. Some techniques are based on gas absorption on high surface amorphous materials, like, e.g., activated carbons,[1] cross-linked polymers,[2] or carbon nanotubes.[3] More selective techniques are based on inclusion of gas-molecules into cavities of crystalline materials leading to molecular complex crystalline phases (generally clathrate phases). The available nanoporous crystalline frameworks can present a large variety of chemical structures. Mostly studied are inorganic frameworks (e.g., zeolites)[4,5] and, more recently, metal-organic frameworks,[6−9] although the high molecular masses of the framework atoms can limit the gas weight uptake. In this respect organic frameworks, i.e., nanoporous organic crystals,[10−13] often referred to as "organic zeolites", could be more promising.

In this paper, we show that the δ crystalline phase of syndiotactic polystyrene (s-PS),[14,15] can be considered as a first case of *polymeric framework*. In fact, already at room temperature, this polymer crystal phase is able to include suitable gas-molecules leading to molecular complex crystalline phases.

It is well-known that s-PS is a polymer which forms molecular complex crystalline phases (both clathrate[15−21] and intercalate[22,23]) with several, mostly aromatic and/or halogenated, guest molecules. By suitable solvent extraction procedures, the guest molecules can be easily removed leading to the nanoporous δ form (monoclinic, space group $P2_1/a$; $a = 1.74$ nm; $b = 1.18$ nm; $c = 0.77$ nm; $\gamma = 117°$; density = 0.98 g/cm^3)[14] with a permanent cavity (of 120−160 Å^3) per 4 monomer units (Figure 1).[15] This low density crystalline framework rapidly absorbs volatile organic molecules, also if present in traces in air or water, eventually leading to host−guest molecular complex phases and hence is promising for applications in chemical separations [24−30] and molecular sensorics.[31−33]

A gas sorption study, in the temperature range 35−55 °C, has shown that the gas sorption capacity of semicrystalline s-PS samples presenting the host δ phase is generally much higher than for amorphous or for other semicrystalline s-PS samples.[34] However, these gravimetric experiments did not give any direct evidence of s-PS/gas clathrate formation, i.e., of an ordered three-dimensional organization of polymer host and gas guest molecules.

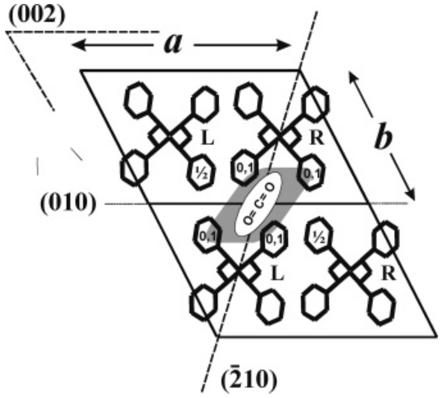

Figure 1. Along *c* view of two adjacent unit cells of the host δ form of s-PS. The shown guest location and orientation into the cavity is based on X-ray diffraction and linear dichroism experiments. Suitable crystallization procedures can lead (002), (010), or ($\bar{2}$10) crystal planes nearly parallel the film surface. Guest release kinetics can be controlled by these uniplanar crystalline phase orientations.

In this communication, we show that gas molecules like for instance butadiene (boiling temperature at atmospheric pressure, $T_b = -5$ °C) and carbon dioxide ($T_b = -78$ °C), also at room temperature, form real clathrate phases with s-PS.

Desorption kinetics at room temperature of butadiene and carbon dioxide, after room-temperature equilibrium uptake (at a pressure of 1 and 15 atm, respectively), from 0.10 mm thick δ-form (filled symbols and thick lines) and α-form (empty symbols and thin lines) s-PS films, are compared in Figure 2. It is clearly apparent that solute uptakes are larger and desorption kinetics are slower, for films presenting the nanoporous host crystalline δ phase. In particular, the CO_2 equilibrium uptake (nearly 4 wt %) is comparable with those observed for to other nanoporous frameworks.[6−9,12,13]

Wide-angle X-ray diffraction (WAXD) patterns of an unoriented δ form film before (A) and after absorption of butadiene (B) are compared in Figure 3. As a consequence of gas

---

* Corresponding author. Telephone: +39-089-969558. Fax: +39-089-969603. E-mail: gguerra@unisa.it.
† Dipartimento di Chimica, Università di Salerno.
‡ Dipartimento di Ingegneria dei Materiali e della Produzione, Università di Napoli "Federico II".

10.1021/ma0618878 CCC: $33.50

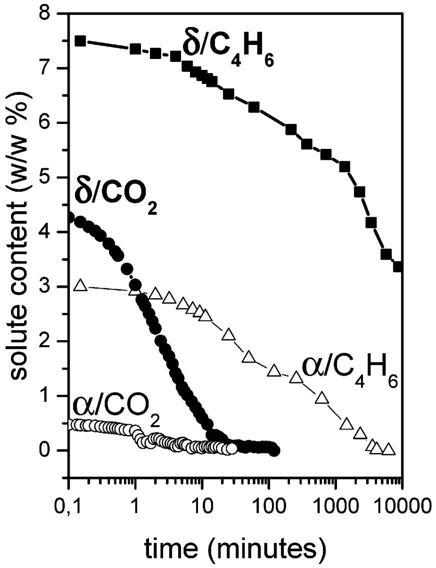

Figure 2. Gas desorption kinetics at room temperature. Butadiene and carbon dioxide desorption after room-temperature uptake, at a pressure of 1 and 15 atm, respectively, from δ-form (filled symbols and thick lines) and α-form (empty symbols and thin lines) s-PS films.

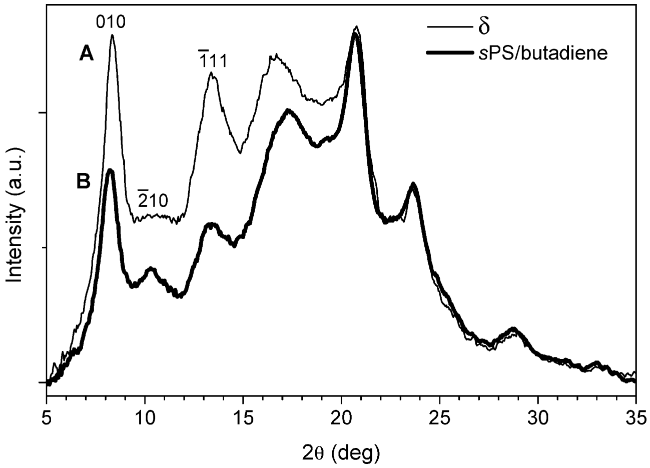

Figure 3. WAXD patterns of polymer/gas clathrates. Patterns collected by an automatic diffractometer (Cu Kα radiation) of an unoriented δ form s-PS film, before (A) and after room-temperature absorption of butadiene (B).

treatment, an intensity decrease of the 010 and $\bar{1}11$ diffraction peaks (at lattice spacing $d \approx 1.06$ and 0.66 nm, respectively) and increase of the $\bar{2}10$ diffraction peak (at lattice spacing $d \approx 0.84$ nm), being diagnostic of guest molecule inclusion into the cavity of the host s-PS phase, are observed.[14] In particular, by assuming a single occupancy of the cavity by the considered gas guest molecules (as observed for most s-PS clathrate phases),[14−19] the observed diffraction intensity changes indicate a location of the guest barycenter close to the center of symmetry of the cavity (and of the unit cell).[14]

However, the information, which can be achieved by WAXD analyses, relative to the guest orientation within the host cavity is poor, due to the generally poor dependence of the calculated diffraction intensity on the guest orientation and to the lack of direct information on the fraction of filled crystalline cavities.[14−19]

More informative are linear dichroism measurements for vibrational peaks of guests of uniaxially oriented δ-form s-PS films. In fact, these kinds of measurements not only allow to establish the orientation of guest molecules with respect to the host chain axis (crystalline c axis), but also allow to discriminate between solute molecules being simply dissolved in the amorphous phase or being guest of the host crystalline δ phase.[35,36]

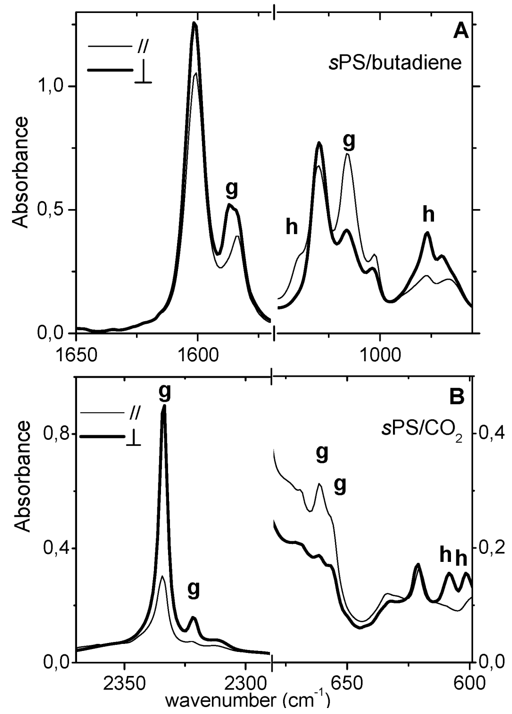

Figure 4. Polarized FTIR spectra of uniaxially stretched polymer/gas clathrates. The spectra are taken with polarization plane parallel (thin lines) and perpendicular (thick lines) to the draw direction, for uniaxially stretched s-PS films ($\lambda \approx 3$), after absorption of butadiene (A) and carbon dioxide (B). The labels **h** and **g** refer to absorbance peaks of helical polymer chains of the host δ phase and of the guest molecules, respectively.

Fourier Transform infrared (FTIR) spectra, taken with polarization plane parallel and perpendicular to the draw direction, of uniaxially stretched (at $\lambda \approx 3$) δ form s-PS films, including butadiene (A) and carbon dioxide (B) are shown in Figure 4. The spectra of Figure 4 have been collected after room-temperature desorption of 5 min for CO_2 and of 20 h for butadiene.

These spectra present dichroic helical peaks of the polymer host (already described in the literature[35,36] and labeled by **h**) as well as dichroic peaks of the gaseous guest molecules (labeled by **g**) for instance at 1015 (||), 1588 ($\perp$) cm^{-1} for butadiene and at 658 (||), 2334 ($\perp$) cm^{-1} for carbon dioxide. On the other hand, the FTIR spectra (not reported) of uniaxially stretched s-PS films, presenting different crystalline phases (e.g., α), show negligible dichroism of peaks of gas molecules, since they are only absorbed in the poorly oriented amorphous phase.

Desorption kinetics of butadiene and carbon dioxide based on the absorbance of the 1015 and 658 cm^{-1} peaks, respectively, calibrated by gravimetric measurements like those of Figure 2, are reported in Figure 5. Guest content has been expressed as number of guest molecules per crystalline cavity (left scale in Figure 5), on the basis of the evaluated crystalline degrees (in the range 35−40%).

As for carbon dioxide, the dichroism of its peaks remains essentially unchanged with guest desorption (e.g., for the 658 cm^{-1} peak, the relative dichroism $LD^r = LD/A^{\text{isotropic}} = 3(A_{||} - A_\perp)/(A_{||} + 2A_\perp) = \approx 0.5$). In good agreement with the very low gas uptake by α form films (lowest curve in Figure 2), this result clearly indicates that already for very short desorption

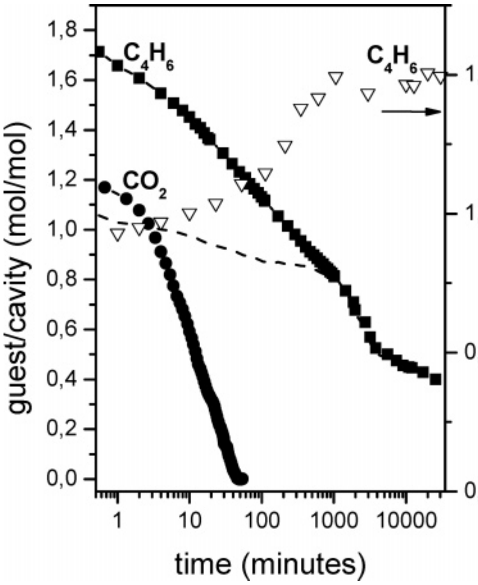

Figure 5. Desorption kinetics of butadiene and carbon dioxide based on absorbance of guest FTIR peaks. Guest content has been expressed as number of guest molecules per crystalline cavity. The dashed curve shows the guest/cavity ratio calculated by excluding molecules absorbed in the amorphous phases. On the right-hand scale is the reduced linear dichroism LD^r, for the 1015 cm^{-1} butadiene peak.

times most CO_2 molecules are guest of the crystalline phase rather than dissolved in the amorphous phase. As for butadiene peaks, their dichroism tends to increase (in absolute value) with guest desorption, gradually reaching plateau values (as shown in Figure 5, for the 1015 cm^{-1} peak). As discussed in detail in previous papers,[25,35] after sorption into semicrystalline nanoporous samples, guest molecules can be partitioned in amorphous and crystalline phases, but the amorphous phase generally loses the guest molecules at a much faster rate than does the crystalline one, and after substantial desorption, most of the residual low-molecular-mass molecules are located in the crystalline phase.

By assuming that the LD^r values, for guest molecules into the crystalline and amorphous phases, correspond to the plateau value and zero, respectively, the amount of butadiene into the host crystalline phase can be easily evaluated (dashed curve in Figure 5). These results clearly indicate that, for short desorption times most of the cavities of the host crystalline δ phase are filled by guest molecules (guest/cavity ratio not far from 1 for both guests). Moreover, as for butadiene, nearly one-half of the cavities is still full after long desorption times (30 000 min).

On the basis of the literature information relative to the transition moment directions for the considered guest molecules[37,38] and by following the procedure described by some of us in previous papers,[35,36] the orientation of the guest molecules with respect to the host *c* axis can be also evaluated.

In particular, the absorbance of the butadiene peaks at 1588 and 1375 cm^{-1}, corresponding to vibrational modes identified as in-plane (B_u symmetry) is larger for light polarization perpendicular to the stretching direction ($LD^r(1588) = -1.2$; $LD^r(1375) = -0.7$). On the other hand, the absorbance of the butadiene peaks at 1015 and 907 cm^{-1}, corresponding to vibrational modes identified as out-of-plane (A_u symmetry) is larger for light polarization parallel to the stretching direction ($LD^r(1015) = +1.5$; $LD^r(907) = +1.6$). Analogously, as for carbon dioxide, the absorbance of the peak at 2349 cm^{-1}, corresponding to the parallel stretching mode (A_{1u} symmetry) is larger for light polarization perpendicular to the stretching direction ($LD^r(2349) = -0.8$), while the absorbance of the peaks at 667 cm^{-1} corresponding to the perpendicular bending mode (E_{1u} symmetry) is larger for light polarization parallel to the stretching direction ($LD^r(667) = +0.5$).

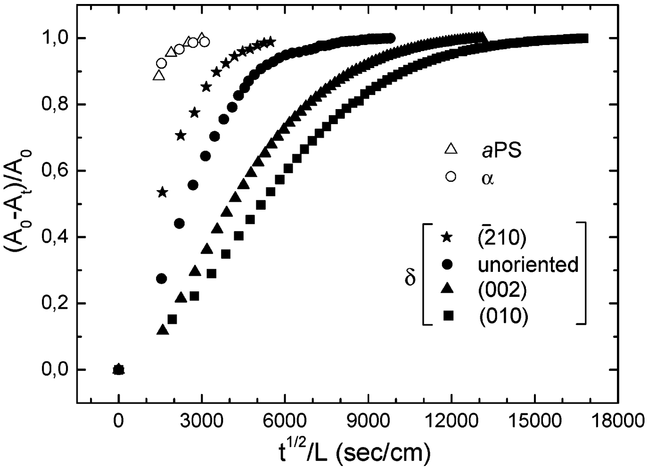

Figure 6. Desorption isotherms of CO_2 at room temperature from polystyrene films: (empty symbols) from amorphous phases of atactic-PS films and of s-PS films presenting the α-form; (filled symbols) from the nanoporous δ-phase of s-PS films, being unoriented or presenting the three different kinds of uniplanar orientation sketched in Figure 1, i.e., (010), $(\bar{2}10)$, or (002).

These results clearly indicate that the molecular planes of butadiene guest molecules as well as the molecular axis of CO_2 guest molecules are nearly perpendicular to the chain axis of the host crystalline phase (as schematically shown in Figure 1, for carbon dioxide).

In summary, combined gravimetric, WAXD and FTIR analyses clearly indicate the formation, also at room temperature, of real s-PS/gas clathrate phases.

The guest release from these s-PS/gas clathrate phases has also been studied for film with different kinds of uniplanar orientation. In fact, for δ form s-PS films, suitable solution or solvent induced crystallization procedures can lead to three different kinds of uniplanar orientation, for which three different crystal planes (010),[39] $(\bar{2}10)$,[40] or (002)[41] (schematically shown in Figure 1) tend to be parallel to the film plane.

Particularly suitable for this kind of study are s-PS/CO_2 clathrate films. In fact, as proved by the guest peak dichroism being high and nearly independent of desorption time (see above), the experimentally observed diffusivities can be considered a good approximation of the diffusivities into the crystalline nanoporous phase.

CO_2 desorption kinetics from 0.05 mm thick s-PS films, at room temperature and atmospheric pressure, are reported in Figure 6. The kinetic curves, presenting the absorbance variations of the 658 cm^{-1} peak $(A_0 - A_t)/A_0$ vs the square root of desorption time divided by film thickness ($\sqrt{t}/L$), can be fitted by means of Fick's model. The results of Figure 6 clearly indicate that the CO_2 diffusivity is larger in the amorphous phases of atactic PS as well as of α-form s-PS films ($D \approx 8.0 \times 10^{-8}$ cm^2/s) while it is reduced of more than an order of magnitude, as a consequence of clathration into the host δ phase (D [δ, unoriented] $\approx 0.7 \times 10^{-8}$ cm^2/s). Moreover the guest diffusivity is largely different for films with different uniplanar orientations, in particular D [δ, (010)] $\approx 0.2 \times 10^{-8} \leq D$ [δ, (002)] $\approx 0.3 \times 10^{-8} < D$ [δ, unoriented] $< D$ [δ, $(\bar{2}10)$] $\approx 1.6 \times 10^{-8}$ cm^2/s.

In agreement with previous molecular dynamics simulations[42,43] and less precise desorption kinetics of 1,2-dichloroethane,[44] the lowest diffusivity has been measured for films with

(010) uniplanar orientation, presenting layers of close-packed enantiomorphous s(2/1)2 helices nearly parallel to the film surface. Moreover, the highest diffusivity has been measured for films with uniplanar orientation of the ($\bar{2}$10) crystalline plane, whose normal forms an angle of only 17.5° with the *a* axis, which was calculated as the δ form crystalline axis of maximum diffusivity.[42] The described kinetics and anisotropy of guest release remain essentially unaltered as a consequence of repeated CO_2 sorption and desorption cycles.

In summary, the present paper shows that several gas molecules can form molecular complex (clathrate) phases with s-PS, by inclusion into its nanoporous host δ phase, thus leading to gas uptake and selectivity comparable to those of other nanoporous materials.[6−9,12,13] Moreover, the gas guest diffusivity is strongly reduced as a consequence of polymer/gas clathrate formation and it can be further reduced by (010) uniplanar orientation of the host crystalline phase.

These transport properties, being unique for polymeric materials, are associated with several practical advantages. In fact, the polymeric host framework can be obtained by a cheap commercial polymer and, due to its macromolecular nature, it is robust (chemical and thermal resistant), easy to process (can be easily shaped as film, fiber, membrane, foam, aerogel, ...) and presents excellent mechanical properties. Hence, polymeric frameworks are suitable candidates as repeated use gas storage and controlled release materials.

Experimental Section

Materials. s-PS was supplied by Dow Chemical under the trademark Questra 101. ^{13}C nuclear magnetic resonance characterization showed that the content of syndiotactic triads was over 98%. The weight-average molar mass obtained by gel permeation chromatography (GPC) in trichlorobenzene at 135 °C was found to be $M_w = 3.2 \times 10^5$ with the polydispersity index, $M_w/M_n = 3.9$.

Amorphous films were obtained by extrusion of the melt with an extrusion head of 200 mm × 0.5 mm. Uniaxially oriented films have been obtained by uniaxial stretching of the extruded ones, at draw ratios λ = final length/initial length ≈ 3, at constant deformation rate of $0.1\ s^{-1}$, in the temperature range 105−110 °C with a Brukner stretching machine. The stretched films, still essentially amorphous, have been crystallized into the nanoporous δ form by exposure for 3 days to CS_2 vapors, followed by treatment under vacuum at 40 °C for other 3 days.

The molecular-complex films with uniplanar (010) and (002) orientations have been obtained by casting from 0.5 wt % solutions, at room temperature from chloroform[39] and at 50 °C from trichloroethylene,[41] respectively. The molecular-complex film with uniplanar ($\bar{2}$10) orientation has been obtained by *o*-xylene diffusion at 50 °C in an unoriented amorphous film.[40]

The unoriented molecular-complex film has been obtained by THF diffusion in γ form films, in turn obtained by acetone treatment of an amorphous film.[45] The unoriented and oriented s-PS molecular-complex phases were transformed into nanoporous δ phases by treatment with carbon dioxide at 200 bar and 40 °C.[46] The residual guest content in the samples, after these extraction procedures, as evaluated by thermogravimetric measurements, was lower than 0.1%.

The α-form films have been obtained from the above-described amorphous films, by annealing at 220 °C for 30 min.

All the considered unoriented and oriented s-PS δ-form films present a degree of crystallinity in the range 30−40%, as measured by the FTIR spectral subtraction procedures, described in ref. 45

WAXD Measurements. Wide-angle X-ray diffraction patterns with nickel filtered Cu Kα radiation were obtained, in reflection, with an automatic Bruker diffractometer. The overall collection time, for the patterns of polymer/gas clathrates of Figure 1, was 30 min.

The degree of the three different kinds of uniplanar orientation for the δ form s-PS films, that is the degree of parallelism of the three crystallographic planes with respect to the film plane, have been formalized on a quantitative numerical basis using Hermans' orientation functions, f_{010}, f_{210}, and f_{002}, where

$$f_{hkl} = (3\overline{\cos^2 x_{hkl}} - 1)/2(1) \tag{1}$$

by assuming $\overline{\cos^2 x_{hkl}}$ as the squared average cosine value of the angle, x_{hkl}, between the normal to the film surface and the normal to the (*hkl*) crystallographic plane. In these assumptions, f_{hkl} is equal to 1 if (*hkl*) planes of all crystallites are perfectly parallel to the plane of the film. The orientation factors for the considered (010), ($\bar{2}$10), and (002) oriented films, evaluated according to the method described in ref 40, are $f_{010} \approx 0.8$, $f_{\bar{2}10} \approx 0.63$, and $f_{002} \approx 0.6$, respectively.

The orientation of the crystalline phase of the uniaxially stretched films is characterized by high degree of parallelism of the chain axes with respect to the stretching direction ($f_c = 0.9$).

FTIR Measurements. Infrared spectra were obtained at a resolution of 2.0 cm^{-1} with a Vector 22 Bruker spectrometer equipped with deuterated triglycine sulfate (DTGS) detector and a KBr beam splitter. The frequency scale was internally calibrated to 0.01 cm^{-1} using a He−Ne laser. Then, 32 or 16 scans were signal averaged to reduce the noise. Polarized infrared spectra were recorded by the use of a SPECAC 12500 polarizer.

Acknowledgment. Financial support of "Ministero dell' Istruzione, dell'Università e della Ricerca" (PRIN 2004) and of "Regione Campania" (Legge 5 and Centro di Competenza per le Attività Produttive) is acknowledged. We thank Florian Müller-Plathe, Pellegrino Musto, Paola Rizzo, and Giuseppe Milano for useful discussions and Rosa Califano for experimental support.

References and Notes

(1) Zhao, X. B.; Xiao, B.; Fletcher, A. J.; Thomas, K. M. *J. Phys. Chem. B* **2005**, *109*, 8880−8888.

(2) Simpson, E. J.; Koros, W. J.; Schechter, R. S. *Ind. Eng. Chem. Res.* **1996**, *35*, 4635−4645.

(3) Penza, M.; Cassano, G.; Aversa, P.; Cusano, A.; Cutolo, A.; Giordano, M.; Nicolais, L. *Nanotechnology* **2005**, *16*, 2536−2547.

(4) Kuznicki, S. M.; Bell, V. A.; Nair, S.; Hillhouse, H. W.; Jacubinas, R. M.; Braunbarth, C. M.; Toby, B. H.; Tsapatsis, M. *Nature (London)* **2001**, *412*, 720−724.

(5) Zecchina, A.; Bordiga, S.; Vitillo, J. G.; Ricchiardi, G.; Lamberti, C.; Spoto, G.; Bjorgen, M.; Lillerud, K. P. *J. Am. Chem. Soc.* **2005**, *127*, 6361−6366.

(6) Eddaoudi, M.; Li, H.; Yaghi, O. M. *J. Am. Chem. Soc.* **2000**, *122*, 1391−1397.

(7) Pan, L.; Adams, K. M.; Hernandez, H. E.; Wang, X.; Zheng, C.; Hattori, Y.; Kaneko, K. *J. Am. Chem. Soc.* **2003**, *125*, 3062−3067.

(8) Kitaura, R.; Seki, K.; Akiyama, G.; Kitagawa, S. *Angew. Chem. Int. Ed.* **2003**, *42*, 428−431.

(9) Millward, A. R.; Yaghi, O. M. *J. Am. Chem. Soc.* **2005**, *127*, 17998−17999.

(10) Soldatov, D. V.; Moudrakovski, I. L.; Ripmeester, J. A. *Angew. Chem. Int. Ed.* **2004**, *43*, 6308−6311.

(11) Blau, W. J.; Fleming, A. J. *Science* **2004**, *304*, 1457−1458.

(12) Atwood, J. L.; Barbour, L. J.; Jerga, A. *Angew. Chem. Int. Ed.* **2004**, *43*, 2948−2950.

(13) Sozzani, P.; Bracco, S.; Comotti, A.; Ferretti, L.; Simonutti, R. *Angew. Chem. Int. Ed.* **2005**, *44*, 1816−1820.

(14) De Rosa, C.; Guerra, G.; Petraccone, V.; Pirozzi, B. *Macromolecules* **1997**, *30*, 4147−4152.

(15) Milano, G.; Venditto, V.; Guerra, G.; Cavallo, L.; Ciambelli, P.; Sannino, D. *Chem. Mater.* **2001**, *13*, 1506−1511.

(16) Chatani, Y.; Shimane, Y.; Inagaki, T.; Ijitsu, T.; Yukinari, T.; Shikura, H. *Polymer* **1993**, *34*, 1620−1624.

(17) Chatani, Y.; Inagaki, T.; Shimane, Y.; Shikuma, H. *Polymer* **1993**, *34*, 4841−4845.

(18) De Rosa, C.; Rizzo, P.; Ruiz de Ballesteros, O.; Petraccone, V.; Guerra, G. *Polymer* **1999**, *40*, 2103−2128.

(19) Tarallo, O.; Petraccone, V. *Macromol. Chem. Phys.* **2005**, *206*, 672−679.

(20) Stegmaier, P.; De Girolamo Del Mauro, A.; Venditto, V.; Guerra, G. *Adv. Mater.* **2005**, *17*, 1166−1168.

(21) Uda, Y.; Kaneko, F.; Tanigaki, N.; Kawaguchi, T. *Adv. Mater.* **2005**, *17*, 1846−1850.

(22) Petraccone, V.; Tarallo, O.; Venditto, V.; Guerra, G. *Macromolecules* **2005**, *38*, 6965−6971.

(23) Tarallo, O.; Petraccone, V.; Venditto, V.; Guerra, G. *Polymer* **2006**, *47*, 2402−2410.

(24) Manfredi, C.; Del Nobile, M. A.; Mensitieri, G.; Guerra, G.; Rapacciuolo, M. *J. Polym. Sci., Polym. Phys. Ed.* **1997**, *35*, 133−140.

(25) Musto, P.; Manzari, M.; Guerra, G. *Macromolecules* **1999**, *32*, 2770−2776.

(26) Guerra, G.; Milano, G.; Venditto, V.; Musto, P.; De Rosa, C.; Cavallo, L. *Chem. Mater.* **2000**, *12*, 363−368.

(27) Musto, P.; Mensitieri, G.; Cotugno, S.; Guerra, G.; Venditto, V. *Macromolecules* **2002**, *35*, 2296−2304.

(28) Sivakumar, M.; Yamamoto, Y.; Amutharani, D.; Tsujita, Y.; Yoshimizu, H.; Kinoshita, T. *Macromol. Rapid Commun.* **2002**, *23*, 77−79.

(29) Uda, Y.; Kaneko, F.; Kawaguchi, T. *Macromol. Rapid Commun.* **2004**, *25*, 1900−1904.

(30) Daniel, C.; Alfano, D.; Venditto, V.; Cardea, S.; Reverchon, E.; Larobina, D.; Mensitieri, G.; Guerra, G. *Adv. Mater.* **2005**, *17*, 1515−1518.

(31) Mensitieri, G.; Venditto, V.; Guerra, G. *Sens. Actuators B* **2003**, *92*, 255−261**.**

(32) Giordano, M.; Russo, M.; Cusano, A.; Cutolo, A.; Mensitieri, G.; Nicolais, L. *Appl. Phys. Lett.* **2004**, *85*, 5349−5351.

(33) Giordano, M.; Russo, M.; Cusano, A.; Mensitieri, G.; Guerra, G. *Sens. Actuators, B* **2005**, *109*, 177−184.

(34) Larobina, D.; Sanguigno, L.; Venditto, V.; Guerra, G.; Mensitieri, G. *Polymer* **2004**, *45*, 429−436.

(35) Albunia, A. R.; Di Masi, S.; Rizzo, P.; Milano, G.; Musto, P.; Guerra, G. *Macromolecules* **2003**, *36*, 8695−8703.

(36) Albunia, A. R.; Milano, G.; Venditto, V.; Guerra, G. *J. Am. Chem. Soc.* **2005**, *127*, 13114−13115.

(37) Arnold, B. R.; Balaji, V.; Downing, J. W.; Radziszewski, J. G.; Fisher, J. J.; Michl, J. IR *J. Am. Chem. Soc.* **1991**, *113*, 2910−2919.

(38) Herzberg, G. *Molecular spectra and molecular structure*; Krieger Publ. Corp.: Malabar, FL, 1991; p 272.

(39) Rizzo, P.; Lamberti, M.; Albunia, A.; Ruiz de Ballesteros, O.; Guerra, G. *Macromolecules* **2002**, *35*, 5854−5860.

(40) Rizzo, P.; Spatola, A.; De Girolamo Del Mauro, A.; Guerra, G. *Macromolecules* **2005**, *38*, 10089−10094.

(41) Rizzo, P.; Costabile, A.; Guerra, G. *Macromolecules* **2004**, *37*, 3071−3076.

(42) Milano, G.; Guerra, G.; Müller-Plathe, F. *Chem. Mater.* **2002**, *14*, 2977−2982.

(43) Tamai, Y.; Fukuda, M. *J. Chem. Phys.* **2004**, *121*, 12085−12093.

(44) Venditto, V.; De Girolamo Del Mauro, A.; Mensitieri, G.; Milano, G.; Musto, P.; Rizzo, P.; Guerra, G. *Chem. Mater.* **2006**, *18*, 2205−2210.

(45) Albunia, A. R.; Musto, P.; Guerra, G. *Polymer* **2006**, *47*, 234−242.

(46) Reverchon, E.; Guerra, G.; Venditto, V. *J. Appl. Polym. Sci.* **1999**, *74*, 2077−2082.

MA0618878